



Activated carbon-mediated base hydrolysis of alkyl bromides

Hsin-Se Hsieh, Joseph J. Pignatello*

Department of Environmental Sciences, The Connecticut Agricultural Experiment Station, 123 Huntington Street, P.O. Box 1106, New Haven, CT 06504-1106, United States

ARTICLE INFO

Article history:

Received 11 January 2017
Received in revised form 10 March 2017
Accepted 3 April 2017
Available online 5 April 2017

Keywords:

Activated carbon
Methyl bromide
Alkyl bromide
Base hydrolysis
Anion exchange

ABSTRACT

Activated carbon (AC) is widely used as an adsorbent in water and air purification, but recent studies show that AC can also mediate chemical reactions at ambient temperature, including electron-transfer, redox, free radical, and dehydrohalogenation. Here, we expand the repertoire of such reactions to S_N2 base hydrolysis of alkyl bromides. Detailed studies were carried out on the quarantine and pre-shipment fumigant, methyl bromide (MeBr), whose removal from fumigation vent streams is sought due to its ozone-depleting potential. Mixed with a 1 M solution of NaOH, ACs are effective adsorbents, but also participate in hydrolysis of MeBr to bromide, methanol, and dimethyl ether. MeBr decay is first order in MeBr and obeys a two-term rate law corresponding to aqueous- and adsorbed-state reactions. The adsorbed-state reaction is, *i*) unassisted by surface groups, as shown by cycling experiments; *ii*) 0.83 order in aqueous hydroxide concentration suggesting participation of adsorbed hydroxide; *iii*) accelerated by pre-adsorption of quaternary ammonium surfactants, which also shift the zeta potential into the positive region; and *iv*) inhibited by competing inert anions in the order of their chromatographic retention time on ion-exchange resins: $Br^- < NO_3^- < ClO_4^-$. The results support an anion exchange mechanism in which hydroxide is attracted to positive sites on the carbon. Normalized to aqueous-phase rate constants, adsorbed-state rate constants for RBr followed the order, R = methyl > ethyl > propyl.

© 2017 Elsevier B.V. All rights reserved.

1. Introduction

Activated carbon (AC) is widely used to separate or concentrate hazardous organic contaminants from air and water waste streams due to its strong adsorptive properties. The choice of treatment for reuse of the AC depends on the degree of resistance of the adsorbed contaminants to desorption and/or degradation. The options may include degradation during thermal regeneration of the carbon; desorption followed by degradation in a separate step; and degradation *in situ* by the addition of appropriate reagents. For the *in situ* option, the carbon itself may or may not participate in the reaction. If it does not, the adsorbed-state contaminant may be less reactive or unreactive toward reagents in the fluid phase, and thus desorption may be rate-limiting to degradation. Pyrogenic substances related to AC, such as chars and soots from fires and fossil fuel combustion ("black carbon"), are widely distributed in the environment and known to play important roles in adsorbing and transporting organic pollutants [1,2]. The susceptibility of black carbon-adsorbed pollutants to carbon-mediated reactions is

an important consideration in regard to their fate and distribution in the environment.

Besides acting as adsorbents, AC and other pyrogenic carbonaceous materials are reported to be capable of mediating various reactions including electron-transfer [3], oxidation-reduction [4], free radical polymerization [5], dehydrogenation [6], and dehydrohalogenation [7–9]. Mediation is thought to be achieved through special properties of the graphene-like surface (such as its electrical conductivity), by virtue of nanopore confinement, or through the involvement of surface functional groups. For example, Pereira et al. [10] proposed that surface carbonyl/quinone groups were responsible for the catalytic performance of ACs at elevated temperature toward oxidative dehydrogenation of ethylbenzene. Amezquita-Garcia et al. [11] proposed that surface hydroquinone/quinone groups mediate the room-temperature reduction of nitroaromatic compounds on AC fibers by sulfides (H_2S/HS^-) by acting as electron shuttles. Xu et al. proposed that graphite *via* its electrical conductivity mediates short-range electron transfer between sulfides and nitroaromatic compounds [12] and long-range electron transfer between sulfides and nitroglycerine [3].

A role for AC in hydrolytic reactions, which is the subject of the present study, has also been suggested. Deprotonated surface groups, such as $-CO_2^-$ and $-O^-$, were implicated in catalyzing the

* Corresponding author.

E-mail addresses: Joseph.Pignatello@ct.gov, joseph.pignatello@yale.edu
(J.J. Pignatello).

dehydrochlorination of 1,1,2,2-tetrachloroethane at low adsorbed concentration (1.25 mg/g-AC) in neutral or alkaline solution [9]. In contrast, Heilmann et al. [13] found that base hydrolysis of the explosive, hexahydro-1,3,5-trinitro-1,3,5-triazine (RDX) at higher adsorbed concentration (187 mg/g-AC), was slower than in the aqueous-phase reaction, despite that the final yields of two major products, formate and nitrite, were virtually the same. They suggested that RDX in the adsorbed state was less reactive or inert to base hydrolysis. Gan et al. [14] studied the neutral hydrolysis of methyl bromide and methyl iodide adsorbed to several ACs but focused on practical issues rather than mechanistic issues related to AC participation. Previous research has shown that base-catalyzed hydrolysis of contaminants partitioned into dissolved humic substances occurs but is retarded compared to the truly dissolved state due to repulsion of hydroxide ion (OH^-) by the negatively charged humic backbone [15]. Since AC surfaces are ordinarily net negatively charged at high pH, it may be expected on first consideration that AC likewise would suppress base hydrolysis by passive sequestration of the contaminant *via* adsorption.

Methyl bromide (MeBr, CH_3Br) is a fumigant and chemosterilant that has been banned under the Montreal Protocol for most uses due to its ozone-depleting potential. The Montreal Protocol, however, allows exemptions for the use of MeBr as a quarantine and pre-shipment (QPS) fumigant, among other critical uses [16]. In a typical QPS fumigation, the commodity is treated in a chamber and the spent MeBr vapors are vented to the atmosphere. Development of technologies for removal and destruction of MeBr in fumigation vent streams is critical for sustaining the QPS exemption. MeBr is also an attractive fumigant for decontaminating buildings exposed to biological contaminants, such as spores of *Bacillus anthracis* or its surrogates [17]. Because MeBr is toxic to humans, there is a need to effectively capture and destroy MeBr emissions resulting from this potential application also. Previous research has shown that ACs can effectively and economically adsorb MeBr from fumigation vent streams. For example, in a recent full-scale test the practical adsorption capacity of an AC was determined to be 4.83% by weight at an initial concentration of 41,000 ppmv at 27 °C and 75% RH [17]. Meanwhile, studies have been undertaken on methodology to regenerate the laden AC, including thermal desorption [18], electrolysis [19], and wet degradation [14,20]. Thermal desorption leaves a product that still must be disposed, since reuse of the desorbed MeBr is regarded as undesirable due to carry-over of other volatiles from the fumigated commodity [18]. Electrolysis is effective but slow.

MeBr is susceptible to attack by various nucleophiles (Nu; e.g., thiosulfate, sulfide, hydroxide, etc.), releasing bromide ion and the methylated nucleophile according to [21,22],



Thiosulfate reacts rapidly in aqueous solution, but produces methyl thiosulfate, whose toxic effects are not well characterized. Water hydrolysis produces methanol but is too slow to be practical and produces HBr, which has to be neutralized because it is highly corrosive. We present here an investigation of base hydrolysis for *in situ* degradation of AC-trapped MeBr. Hydroxide is 10^4 -times more nucleophilic than water and produces methanol as the major product. To our knowledge there are no reported studies addressing base hydrolysis of MeBr or other alkyl bromides in AC systems, although base-catalyzed dehydrohalogenation reactions have been investigated [7,8]. We expected to find that hydrolysis would be limited by diffusion into the aqueous phase, but on further investigation found that MeBr hydrolysis occurs in both the adsorbed and dissolved states. The objective of the present study was to understand the surface-mediated component of base hydrolysis.

2. Material and methods

2.1. Materials

Two batches of WPX powdered AC (325 mesh) (hereafter, "WPX-1" and "WPX-2") and Centaur NDS 20 × 50 mesh granular AC were received from Calgon Carbon (Moon Township, PA). Darco 4 × 12 mesh granular AC and RO 0.8 mm pellets were purchased from Sigma Aldrich (St. Louis, MO). Surface area and porosity were characterized by N_2 adsorption (Autosorb-1C, Quantachrome Instruments) after outgassing for at least 4 h at 200 °C to pass the instrument criterion. The BET surface areas (11 point, $P/P_0 = 0.05–0.3$) were found to be 871 (WPX-1), 754 (WPX-2), 789 (Centaur), 390 (Darco), and 895 (RO) m^2/g . Total pore volumes (at $P/P_0 = 0.995$) were 0.63 (WPX-1), 0.54 (WPX-2), 0.46 (Centaur), 0.48 (Darco), 0.71 (RO) cm^3/g . Anion exchange capacity was determined by a standard method [23] except that perchlorate (NaClO_4) was used to displace adsorbed bromide; details are given in the Supplementary Information (SI) section. The method for determining electrokinetic (zeta) potential of AC particles is provided in the SI.

Methyl bromide (MeBr) was obtained in pure form from Triest AG Group (Greenville, NC). Ethyl bromide (EtBr, 98%), 1-bromopropane (PrBr, 99%), sodium hydroxide pellets (98%), sodium bromide (99.5%), tetrabutylammonium chloride (TBAC, 95%), and ethyl acetate (99.9%) were purchased from Fisher Scientific (Pittsburgh, PA); cetyltrimethylammonium chloride (CTAC, 99%) from J.T. Baker (Phillipsburg, NJ); sodium perchlorate (ACS grade) from Sigma-Aldrich; and sodium nitrate (ACS grade) from Mallinckrodt (St. Louis, MO). Aqueous solutions were prepared with water purified by a Millipore Milli-Q Integral 10 system.

2.2. Phase partitioning

A Tedlar sample bag (SKC Inc.) was used to transfer MeBr (b.p., 4 °C) from its tank to reaction vessels. The dimensionless Henry's law constant, K_H ($\text{L}_{\text{aq}}/\text{L}_g$) was determined as described in the SI. For adsorption, different amounts of MeBr gas were injected into 22-mL vials containing AC (0.2 g) and water (4 mL) through the PTFE-lined silicone cap septum. After equilibration with gentle mixing at the desired temperature for 2 h, 30 μL of the headspace was withdrawn by gastight syringe and injected into a gas chromatograph equipped with a flame ionization detector (GC-FID) for analysis. External standards were prepared by injecting MeBr into empty vials. The aqueous concentration was calculated based on the temperature-specific K_H . The adsorbed MeBr concentration, C_{AC} , was calculated as the difference between the spiked amount (M_{tot}) and the amounts remaining in the gaseous (M_g) and aqueous (M_{aq}) phases by:

$$C_{\text{AC}} = \frac{M_{\text{tot}} - M_{\text{aq}} - M_g}{Q_{\text{AC}}} = \frac{M_{\text{tot}} - \frac{V_{\text{aq}}C_g}{K_H} - V_gC_g}{Q_{\text{AC}}} \quad (2)$$

where Q_{AC} is the mass of AC, V_{aq} and V_g are the volumes of water and headspace, and C_g is the measured headspace concentration.

The methods for constructing desorption isotherms of MeBr and sorption isotherms of cetyltrimethylammonium cation (CTA^+) on AC are provided in the SI.

2.3. Hydrolysis

In a typical experiment, MeBr gas (1.5 mL, $\sim 5.5 \pm 0.1$ mg, determined gravimetrically) was injected into each of 5-mL replicate septum-sealed vials containing 0.5 g AC, and the vials equilibrated at room temperature for 30 min to adsorb the dosed MeBr. The vials were chilled at -20°C overnight to condense MeBr vapors in the headspace and then 1 mL of 0.98–1.0 M NaOH was added and the

pierced septum replaced. Other amounts and volumes were used in select experiments. The vials were then incubated at constant temperature in an oven ($\pm 1^\circ\text{C}$) for predetermined times. To extract MeBr, vials were pre-chilled at -20°C for at least 30 min and 2 mL of ethyl acetate was added, followed by vortex-mixing for 5 min and centrifugation for 3 min at room temperature. Based on the rate constant at 23°C , MeBr hydrolysis was much less than 1% during this operation. For experiments with EtBr and PrBr, the methodology was the same as for MeBr except: 5 μL of the neat liquid were injected and pre-equilibrated at room temperature for 30 min before adding the hydroxide solution; EtBr was extracted by ethyl acetate; and PrBr was extracted by toluene. To evaluate the separate effects of individual cationic surfactants or competitive salts, either the surfactant or the salt was first dissolved in 1 M NaOH before adding the NaOH solution into the vials to initiate hydrolysis. To evaluate the combined effect of cationic surfactant and a salt, the salt stock solution was added last to avoid precipitation of the surfactant by the salt.

Base hydrolysis of MeBr in aqueous solution without AC was determined according to a published procedure [24] by adding 20 μL of MeBr stock solution in acetone (1.745 g in 10 mL) into each of several replicate 2-mL vials containing 2 mL of 1 M NaOH. After vortex-mixing, the vials were placed in an inverted position in an incubator at the desired temperature. At predetermined times, 1 mL of liquid from a sacrificed replicate was transferred by gastight syringe to another vial containing 0.8 mL ethyl acetate and the mixture shaken. The organic layer was then retained for analysis of MeBr.

To test the recyclability of AC, experiments were performed on RO and WPX-1 for determining rates and products, respectively. The rate studies were conducted over five cycles of MeBr degradation, each done according to the typical method described above using a separate batch for each cycle number. The batch used for the $(n+1)^{\text{th}}$ cycle rate measurement was previously treated n times by, a) adsorbing 4 wt% MeBr, b) adding 1 M NaOH solution and incubating for 3 h at 55°C to achieve complete hydrolysis, and c) decanting the liquid and washing the carbon three times with 6-times its weight with water. After the n^{th} treatment, it was washed twice more with water and dried at 105°C for 8 h in preparation for the $(n+1)^{\text{th}}$ cycle rate measurement. The product studies were done over 4 cycles in a system containing WPX-1 (0.2 g) and 1 M NaOH solution (4 mL) which was dosed sequentially. Each dose was ~ 14.5 mg MeBr and the incubation was for 3 h at 55°C . The cumulative production of bromide and methanol was measured in the supernatant liquid after each cycle.

2.4. Analyses

To determine alkyl bromides, the solvent extract was filtered through a $0.2\text{ }\mu\text{m}$ Nylon filter, and 1.0 μL analyzed by gas chromatography-flame ionization detection (GC-FID) (Agilent 6890) on an Agilent GS-Q PLOT column ($30\text{ m} \times 0.535\text{ mm}$) with 20 mL min^{-1} H_2 as carrier gas, 150°C inlet temperature, and 300°C detector temperature. For MeBr, the initial oven temperature of 100°C was held for 6 min, then ramped at 40 K per min to 200°C where it was held for 4 min. External calibration standards were prepared by dissolving different amounts of MeBr into GC vials containing ethyl acetate (2 mL). The extraction recovery of MeBr from WPX-1 using ethyl acetate was $73.6 \pm 1.0\%$, calculated from triplicate samples; samples were corrected for this recovery. For EtBr, the oven setting was 120°C held for 1 min, then ramped at 10 K per min to 210°C where it was held for 3 min. For PrBr, the oven setting was 120°C held for 1 min, then ramped at 20 K per min to 170°C where it was held for 3 min and ramped at 20 K per min to 220°C where it was held for 4 min. For methanol, the external calibration standards were prepared by adding different amounts

of methanol into an AC-water mixture, followed by ethyl acetate extraction and analysis as above. Bromide concentration was determined using a bromide ion selective electrode (Cole-Parmer) after diluting, centrifuging, and filtering the incubated samples; sodium nitrate was used to adjust ionic strength. The yield of bromide from degradation experiments was 95% of theoretical, indicating that the leakage of MeBr during operations was negligible. Other products (methyl chloride and dimethyl ether) were identified by GC-mass spectrometry (GC-MS) (Agilent 6890GC coupled with 5973MSD) on a Restek Rt-QS-bond column ($15\text{ m} \times 0.25\text{ mm}$) with a flow of 1 mL min^{-1} He. The scan range was m/z 20–100.

2.5. Rate law

We consider hydrolysis in a three-phase system containing aqueous alkali (aq), AC (AC), and headspace (g). Assuming an $\text{S}_{\text{N}}2$ reaction with hydroxide ion predominating over water as the attacking nucleophile, the loss of total MeBr mass, M_{tot} , contained in a sealed vessel may be expressed by a two-term rate law (Eq. (3)):

$$-\frac{dM_{\text{tot}}}{dt} = k_{\text{obs}}M_{\text{tot}} = \left\{ k_{\text{aq}}[\text{OH}^-]_{\text{aq}} \cdot f_{\text{aq}} + k_{\text{AC}}[\text{OH}^-]_{\text{AC}} \cdot f_{\text{AC}} \right\} M_{\text{tot}} \quad (3)$$

where k_{obs} is the overall pseudo first-order rate constant (h^{-1}); k_{aq} ($\text{L mol}^{-1} \text{h}^{-1}$) and k_{AC} ($\text{kg mol}^{-1} \text{h}^{-1}$) are the second-order rate constants; f_{aq} and f_{AC} are the mass fractions of MeBr in the aqueous and adsorbed phases; $[\text{OH}^-]_{\text{aq}}$ (mol L^{-1}) is the aqueous-phase hydroxide concentration; and $[\text{OH}^-]_{\text{AC}}$ (mol kg^{-1}) is the adsorbed hydroxide concentration available for reaction with adsorbed MeBr. If mass transfer of OH^- is not rate-limiting, then when $[\text{OH}^-]_{\text{aq}}$ is constant, $[\text{OH}^-]_{\text{AC}}$ is also constant, and k_{obs} can be written:

$$k_{\text{obs}} = k_{\text{obs,aq}} \cdot f_{\text{aq}} + k_{\text{obs,AC}} \cdot f_{\text{AC}} \quad (4)$$

where $k_{\text{obs,aq}}$ and $k_{\text{obs,AC}}$ are the observed pseudo first-order rate constants for base hydrolysis in the respective phases. If mass transfer of MeBr between the phases is not rate limiting, f_{AC} and f_{aq} can be expressed by,

$$f_{\text{AC}} = \frac{M_{\text{tot}} - C_{\text{aq}}(V_{\text{aq}} + V_{\text{g}}K_{\text{H}})}{M_{\text{tot}}} \quad (5)$$

$$f_{\text{aq}} = \frac{C_{\text{aq}}V_{\text{aq}}}{M_{\text{tot}}} \quad (6)$$

where V_{g} and V_{aq} are the gas and liquid volumes (L), C_{aq} is the aqueous phase concentration (mol L^{-1}), and K_{H} ($= C_{\text{g}}/C_{\text{aq}}$) is the dimensionless air-water (Henry's law) constant. In all cases, V_{aq} represents the total volume of water in the vessel, both intraparticle and interparticle.

WPX-1 powdered AC was used to investigate mechanism in detail and the mechanistic hypotheses were tested on other carbons and alkyl bromides later in the study.

3. Results and discussion

3.1. Partitioning behavior

The measured Henry's law constant for MeBr, plotted against $1/T$, ranged from 0.26 ± 0.01 at 293 K to 0.60 ± 0.05 at 328 K (Fig. 1a). The slope, which corresponds to the enthalpy of air-to-water transfer, $\Delta_{\text{a-w}}H$, is $-20.1 \pm 0.6\text{ kJ/mole}$, a value somewhat lower than the literature value of $-25.5 \pm 1.9\text{ kJ/mole}$ obtained by re-analysis of data assembled from several sources [25].

Fig. 1b shows the 2-h adsorption isotherms of MeBr in a WPX-1/water system at different T between 20 and 55°C . The contact

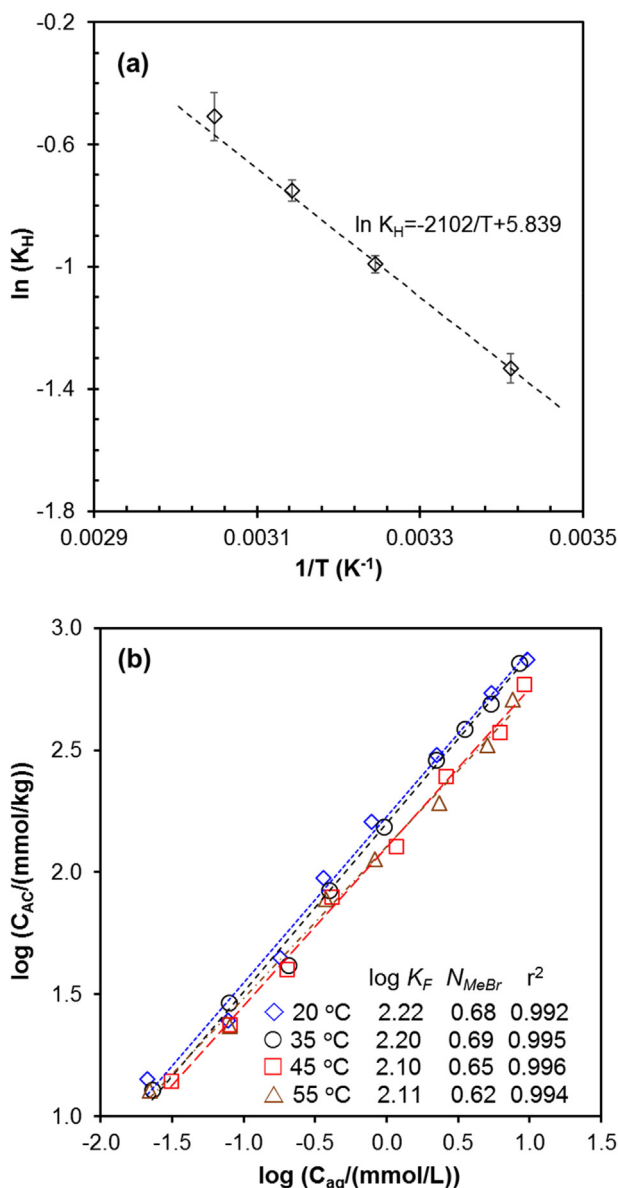


Fig. 1. (a) Henry's law constant of MeBr in water. The dashed line represents the linear regression of data at different temperatures. (b) Adsorption isotherms of MeBr between WPX-1 and water and the corresponding Freundlich model fits at different temperatures.

time was chosen on the basis of a compromise among practical considerations of technological relevance to the problem at hand, approach to equilibrium (<10% additional uptake was observed between 2 and 4 h), and interference from neutral hydrolysis which increases with time and temperature. Adsorption appeared to be reversible using a 2-h contact time (Fig. S1). The adsorption data for WPX-1 were well fit by the simple Freundlich model (Eq. (7)).

$$C_{AC} = K_{F,MeBr} C_{aq}^{N_{MeBr}} \quad (7)$$

where $K_{F,MeBr}$ and N_{MeBr} are the Freundlich adsorption and linearity coefficient, respectively. The Freundlich parameters obtained by linear regression of the log-transformed data set are given in Fig. 1b. As T increases, $\log K_{F,MeBr}$ declines slightly from 2.22 to 2.11 and the isotherm becomes slightly less linear (N_{MeBr} from 0.68 ± 0.02 to 0.62 ± 0.02). The nonlinearity of the isotherm means that retention of MeBr by AC will increase as hydrolysis proceeds and as the fumigant vent stream concentration declines over time. For example, at 20 °C and fixed solid-to-liquid ratio (0.5 g/mL), a decrease in

the adsorbed concentration from 5% to 0.5%, will cause an increase in the distribution ratio ($K_d = C_{AC}/C_{aq}$) from 100 to 286 L kg⁻¹, and a decrease in the f_{aq} from 1.96% to 0.7%. Thus, the relative contributions of reaction in the aqueous and solid states will depend on concentration, a factor that must be considered in interpreting kinetic data. Adsorption by WPX-1 is more favorable in the absence of water by about one order of magnitude due to alleviation of competition by water (Fig. S2).

3.2. Hydrolysis kinetics

The values of $k_{obs,aq}$ in 1 M NaOH in the absence of AC for different T in the range 23–55 °C were obtained from the pseudo first-order rate plots (Fig. S3). An activation energy E_a of 63.9 ± 2.3 kJ/mol is calculated from the Arrhenius plot shown in Fig. 2.

To investigate the contribution of base hydrolysis of MeBr in the sorbed state, we chose an initial MeBr loading rate on WPX-1 of 0.011 g/g and a solid-to-liquid ratio of 0.5 g/mL. The employed ratio, which was a practical upper limit, resulted in >96% of total MeBr adsorbed based on Eq. (5). Fig. 3 shows the temporal trend of MeBr loss and the appearance of the products, methanol and bromide ion at 55 °C under these conditions. The yield of bromide after 4 h was nearly quantitative, whereas the yield of methanol was ~65%. Other products included dimethyl ether, $(CH_3)_2O$, and chloromethane, CH_3Cl , which were identified by GC-MS (Fig. S4). Dimethyl ether results from nucleophilic substitution by methoxide ion, which comprises ~3% of methanol present in 1 M NaOH, and is a stronger nucleophile than hydroxide [26]. The yield of dimethyl ether increased by an order of magnitude when the reaction mixture was supplemented with 300 mM methanol (Fig. S5). Chloromethane may originate from nucleophilic substitution by chloride impurity in WPX-1. This is supported by the following: (i) the peak corresponding to CH_3Cl appeared in the headspace of MeBr-loaded WPX-1 before water or NaOH solution was added; (ii) the peak intensity varied with the AC used; and (iii) the peak intensity decreased with each cycle of degradation and washing.

The reaction in WPX-1/1 M NaOH systems under conditions of nearly full adsorption ($f_{AC} = 0.89$ –0.99) was pseudo first-order in MeBr concentration (Fig. 4a). Rate constants and other information appear in Table 1. Fig. 4b compares, as a function of MeBr loading rate, the experimental k_{obs} values at 55 °C with the corresponding k_{obs} values predicted by assuming that AC acted merely as an inert sink for MeBr. This comparison clearly supports AC-mediated hydrolysis. First, the predicted k_{obs} is less than the experimental value—at the lower loading rates, by as much as two orders of magnitude. Second, if hydrolysis occurred only in the aqueous phase the predicted k_{obs} would have increased by 8-fold over the range in MeBr loading rate due to sorption nonlinearity, since f_{aq} increased by 8-fold (0.005–0.04). However, the experimental k_{obs} was independent of loading rate between 0.002 and 0.075 g/g AC (k_{obs} , 0.93–0.96 h⁻¹; Table 1).

From the value of $k_{obs,aq}$ at 55 °C in 1 M NaOH in the absence of AC (6.8 ± 0.4 h⁻¹), the pseudo first-order sorbed-state reaction rate constants, $k_{obs,AC}$, can be calculated by using Eq. (4) and the corresponding k_{obs} for different adsorbed MeBr concentrations; they are listed in Table 1. The $k_{obs,AC}$ exhibits a slight dependence on MeBr loading rate, decreasing from 0.91 ± 0.03 h⁻¹ to 0.76 ± 0.09 h⁻¹ as the loading rate increases from 0.002 to 0.075 g/g. The slight decline in $k_{obs,AC}$ with loading rate suggests that the fraction of the adsorbed pool of MeBr actually available to the attacking nucleophile decreases slightly, possibly due to packing effects of the condensed MeBr. The ratio $k_{obs,AC}/k_{obs,aq}$ based on the average $k_{obs,AC}$ in Table 1 (0.87 h⁻¹) is 0.13. However, without knowing $[OH^-]_{AC}$ it is not possible to conclude which second-order rate constant (k_{AC} or k_{aq}) is the larger. Georgi

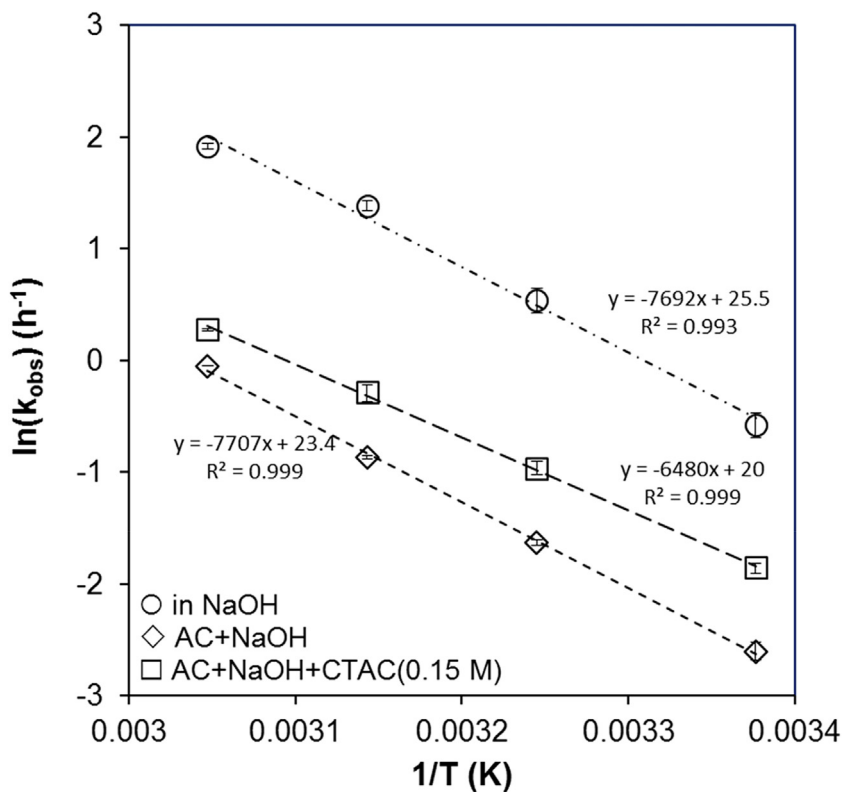


Fig. 2. Arrhenius plot for the hydrolysis of MeBr by 1 M NaOH (1 mL) with or without WPX-1 (0.5 g), and in the presence or absence of cetyltrimethylammonium chloride.

Table 1

Partition data and pseudo first-order reaction rate constants (h^{-1}) for MeBr in a WPX-1/1 M NaOH mixture at 55 °C.

loading rate (g/g)	$k_{\text{obs}}^{\text{a}}$	$f_{\text{gas}}^{\text{b}}$	f_{aq}^{b}	f_{AC}^{b}	$f_{\text{aq}} \cdot k_{\text{obs},\text{aq}}$	$k_{\text{obs},\text{AC}}$	$f_{\text{AC}} \cdot k_{\text{obs},\text{AC}}/k_{\text{obs}}$
0.075	0.95 (0.07) ^c	0.071 (0.012)	0.040 (0.006)	0.889 (0.013)	0.270 (0.044)	0.760 (0.093)	0.71 (0.10)
0.030	0.96 (0.05)	0.044 (0.007)	0.024 (0.003)	0.932 (0.008)	0.160 (0.022)	0.870 (0.060)	0.83 (0.07)
0.011	0.95 (0.08)	0.025 (0.004)	0.014 (0.002)	0.961 (0.004)	0.100 (0.015)	0.890 (0.085)	0.90 (0.10)
0.006	0.95 (0.08)	0.017 (0.002)	0.010 (0.001)	0.973 (0.002)	0.070 (0.008)	0.900 (0.082)	0.93 (0.12)
0.002	0.93 (0.03)	0.009 (0.001)	0.005 (0.0005)	0.986 (0.001)	0.030 (0.003)	0.910 (0.030)	0.96 (0.05)

^a k_{obs} was determined from Fig. 4a.

^b mass fractions calculated from the sorption isotherm and Henry's law constant at 55 °C.

^c standard deviation in parentheses.

Table 2

Pseudo first-order reaction rate constants for base hydrolysis of alkyl bromides in AC/1 M NaOH systems under the condition described in Fig. 4(a).

	MeBr ^a	MeBr ^b	EtBr ^b	PrBr ^b
f_{aq}^{c} $k_{\text{obs}}^{\text{d}}$ (h^{-1})	0.014	0.014	0.0053	0.0017
$k_{\text{obs},\text{aq}}^{\text{d}}$ (h^{-1})	0.95 (0.07)	0.67 (0.01)	0.049 (0.003)	0.0090 (0.0006)
$k_{\text{obs},\text{AC}}^{\text{e}}$	6.8 (0.4)	6.8 (0.4)	1.98 (0.12)	1.09 (0.04)
$k_{\text{obs},\text{AC}}/k_{\text{obs},\text{aq}}$	0.89 (0.09)	0.59 (0.06)	0.039 (0.003)	0.0070 (0.0006)

^a MeBr adsorbed to WPX-1.

^b Alkyl bromides adsorbed to WPX-2.

^c For MeBr, f_{aq} was from Table 1. For EtBr and PrBr, f_{aq} was estimated from K_{ow} [21,30] by $(f_{\text{aq},x} = f_{\text{aq},\text{MeBr}} \times K_{\text{ow},\text{MeBr}}/K_{\text{ow},x})$ where x is EtBr or PrBr.

^d All rate constants were obtained at 55 °C.

^e $k_{\text{obs},\text{AC}} = (k_{\text{obs}} - k_{\text{obs},\text{aq}} \times f_{\text{aq}})/f_{\text{AC}}$, in which f_{AC} was assumed to be 1 for EtBr and PrBr.

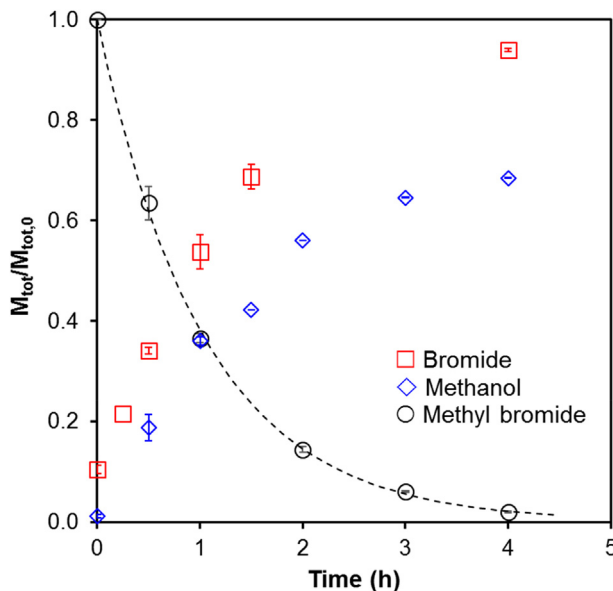


Fig. 3. Hydrolysis of MeBr (5.5 mg) in a system containing WPX-1 (0.5 g) and 1 M NaOH (1 mL) at 55 °C. Greater than 96% of MeBr was adsorbed. Dashed line is the predicted fit to a pseudo first-order rate law. The vertical-axis label is the mole fraction remaining or appearing in the system relative to the initial dosed amount of MeBr.

et al. [15] reported that base-catalyzed dehydrochlorination of γ -hexachlorocyclohexane in aqueous solutions containing humic substances at pH 10 occurred both in the colloidal and truly-dissolved states, with a ratio of pseudo first-order rate constants in the two states of 0.15, a ratio that, interestingly, is similar to the ratio we observed here for WPX-1 (0.13) and not very different than the one for WPX-2 (0.087) (see Table 2).

Fig. 2 shows the variation in k_{obs} over the range 23–55 °C for WPX-1 under conditions where adsorbed-state hydrolysis predominates ($f_{\text{AC}} > 0.96$). The calculated E_a of 64.1 ± 1.3 kJ/mole is not statistically different ($p = 0.454$) from E_a of 63.9 ± 2.3 kJ/mole for the purely aqueous system, indicating transition states of similar structure in the adsorbed and aqueous states.

3.3. Association of hydroxide ion

Base S_N2 hydrolysis of MeBr and other alkyl bromides in aqueous solution is generally first order in $[\text{OH}^-]_{\text{aq}}$ [21]. We may consider the dependence of adsorbed-state hydrolysis rate on $[\text{OH}^-]_{\text{aq}}$. A possible mechanism for the adsorbed-state hydrolysis involves sorption of OH^- . In that case, the $k_{\text{obs,AC}}$ may be expressed in terms of $[\text{OH}^-]_{\text{aq}}$ by substituting the Freundlich isotherm relationship for $[\text{OH}^-]_{\text{AC}}$:

$$k_{\text{obs,AC}} = k_{\text{AC}} [\text{OH}^-]_{\text{AC}} = k_{\text{AC}} \cdot K_{\text{F,OH}^-} [\text{OH}^-]_{\text{aq}}^{N_{\text{OH}^-}} \quad (8)$$

which may be log-transformed to,

$$\log k_{\text{obs,AC}} = \log (k_{\text{AC}} \cdot K_{\text{F,OH}^-}) + N_{\text{OH}^-} \log [\text{OH}^-]_{\text{aq}} \quad (9)$$

where $K_{\text{F,OH}^-}$ and N_{OH^-} represent, respectively, the Freundlich distribution coefficient and the dimensionless linearity exponent for partitioning of OH^- from aqueous solution to the AC surface. If sorbed OH^- participates in adsorbed-state hydrolysis, the value of N_{OH^-} should be less than unity, consistent with the generally non-linear behavior characteristic of most neutral molecules and ions on porous carbons. Fig. 5 plots $\log k_{\text{obs,AC}}$ against $\log [\text{OH}^-]_{\text{aq}}$ for WPX-1. The slope corresponds to N_{OH^-} equal to 0.83 ± 0.03 , which is indeed significantly below 1.

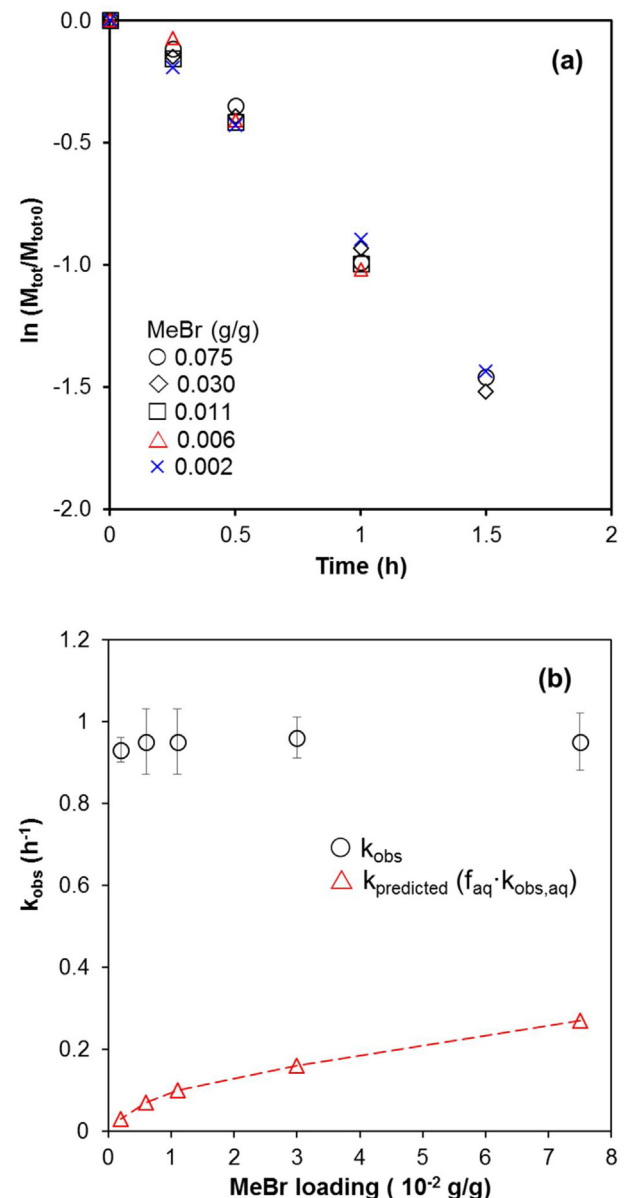


Fig. 4. (a) First-order plots of MeBr decomposition at different loadings on WPX-1. MeBr was first pre-equilibrated with 0.5 g WPX-1, and the reaction was initiated by addition of 1 M NaOH (1 mL) at 55 °C. (b) Comparison of experimental and predicted rate constants under the conditions in (a). The predicted model assumes that AC protected adsorbed MeBr from base hydrolysis.

Quaternary ammonium salts have been used to modify the surface properties of ACs in order to increase their affinity for various anions [27,28]. We hypothesized that, if sorption of OH^- is important, adsorption of quaternary ammonium ions would accelerate base hydrolysis by neutralizing surface charge, thereby reducing electrostatic repulsion of hydroxide ions. Fig. 6 shows that the degradation of MeBr was enhanced by addition of cetyltrimethylammonium chloride (CTAC) to the WPX-1/1 M NaOH mixture. Rate enhancement was also observed for tetrabutylammonium chloride (TBAC) (Fig. S6). At pH 9.7, the electrokinetic (zeta) potential of WPX-1 increases from -38 mV for the pristine carbon to $+8$ mV for the CTA⁺-coated carbon, indicating that CTA⁺ not only neutralizes but reverses the charge (Fig. S7). While zeta potential mainly reflects the outer surface charge of carbon particles, the charge reversal suggests that surface properties of carbon are altered by introducing organocations. Thus, besides reducing repul-

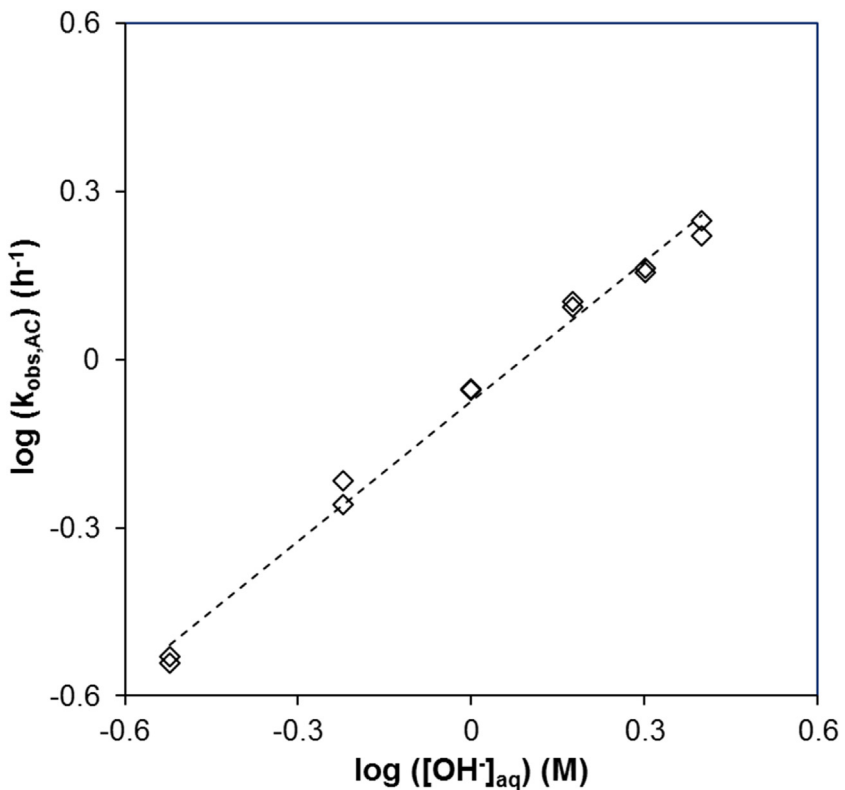


Fig. 5. Effect of aqueous NaOH concentration on $k_{\text{obs,AC}}$ of MeBr hydrolysis at 55 °C. Greater than 96% of MeBr was adsorbed to WPX-1. The slope of the line is the order in $[\text{OH}^-]_{\text{AC}}$, 0.83 ± 0.03 .

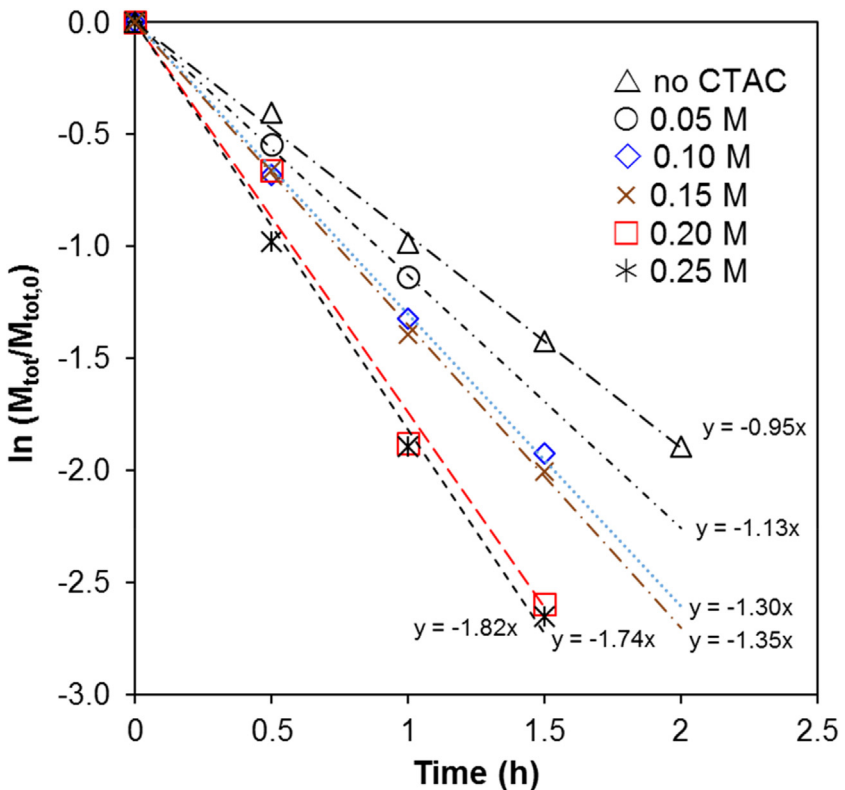


Fig. 6. Effect of cetyltrimethylammonium chloride concentration on the hydrolysis of MeBr adsorbed to 0.5 g WPX-1 in 1 mL of 1 M NaOH at 55 °C. Greater than 96% of MeBr was adsorbed.

sion, another plausible explanation for the rate increase of the adsorbed-state hydrolysis by quaternary ammonium salts is providing additional anion exchange sites that augment $[\text{OH}^-]_{\text{AC}}$. The E_a for hydrolysis on the CTA^+ -coated WPX-1 ($53.8 \pm 1.1 \text{ kJ/mol}$) is lower by about 10.3 kJ/mol than that on the pristine carbon (Fig. 2), suggesting that the CTA^+ coating has a stabilizing effect on the transition state, possibly by affecting solvent re-organization or stabilizing the nascent bromide ion. Thus, the quaternary ammonium salts may positively affect both $[\text{OH}^-]_{\text{AC}}$ and k_{AC} in Eq. (8).

(We addressed two potential artifacts. First, CTAC had no detectable effect on MeBr adsorption from water to WPX-1 (Fig. S8), ruling out an artificial effect caused by CTA^+ displacement of MeBr into solution where the rate constant is greater. Second, although CTAC micelles also accelerated base hydrolysis, their contribution in the WPX-1/1 M NaOH system under our conditions was negligible (see Fig. S9 and discussion in SI).)

If the rate is accelerated by augmentation of $[\text{OH}^-]_{\text{AC}}$, then it may be predicted that addition of a competing, inert anion to the solution would oppose the trend by inhibiting adsorption of OH^- . The degree of inhibition would depend on the anion and its concentration, subject to the thermodynamics of anion exchange between the AC and liquid states. Fig. 7 shows the effects of different salts (0.2 M NaBr , NaNO_3 , or NaClO_4) on the rate of total MeBr loss in the WPX-1/1 M NaOH system. The individual salts at 0.2 M do not react with MeBr [22], nor do they affect aqueous hydrolysis (Fig. S10). However, these salts did, indeed, inhibit hydrolysis in the WPX-1/1 M NaOH systems. Inhibition is generally greater for the CTA^+ -coated WPX-1 than pristine WPX-1 (Fig. 7b), but in both cases inhibition follows the order, $\text{Br}^- < \text{NO}_3^- < \text{ClO}_4^-$. This order is the same as the order in chromatographic elution retention time on Type I and Type II quaternary ammonium ion-exchange resins [29], which reflects anion polarizability. Thus, MeBr hydrolysis is inhibited apparently because these anions displace interfacial OH^- .

3.4. Extension to other carbons and alkyl bromides

To determine if the behavior can be generalized, we studied three granular ACs in comparison with the two different batches of the powdered AC, WPX-1 and WPX-2 (Fig. 8). The k_{obs} in the absence of additives varied in the range $0.67–0.95 \text{ h}^{-1}$ among the carbons. In all cases, CTAC accelerated hydrolysis while NaClO_4 inhibited hydrolysis. The greater the AC surface area, the greater the acceleration by CTAC; for example, k_{obs} of RO 0.8 mm ($\text{SA} = 895 \text{ m}^2/\text{g}$) increased by 114%, whereas k_{obs} of Darco 4 \times 12 ($\text{SA} = 390 \text{ m}^2/\text{g}$) increased by only 47%. Sorption capacity for CTA^+ —and by inference, anion exchange capacity for hydroxide—is expected to trend with surface area.

Reactions were also carried out with other alkyl bromides. Table 2 compares rate constants for MeBr , EtBr , and PrBr in the aqueous and sorbed states. The $k_{\text{obs},\text{aq}}$ decreases in the order $\text{MeBr} > \text{EtBr} > \text{PrBr}$ due to a combination of steric and electronic effects at the carbon center [21]. The $k_{\text{obs},\text{AC}}$ decreases in the same order, but more steeply than for $k_{\text{obs},\text{aq}}$. Hence, $k_{\text{obs},\text{AC}}/k_{\text{obs},\text{aq}}$ follows the order $\text{MeBr} (0.087) > \text{EtBr} (0.020) > \text{PrBr} (0.0060)$.

3.5. Mechanism of AC-mediated base hydrolysis of methyl bromide

Hydrolysis of adsorbed MeBr can occur by direct reaction with sorbed hydroxide ion or with a surface hydroxyl group deprotonated by hydroxide in a prior step. Given the propensity for MeBr to react with nucleophiles by an $\text{S}_{\text{N}}2$ rather than $\text{S}_{\text{N}}1$ mechanism, the surface hydroxyl pathway would result in methylation of the surface hydroxyl groups, would compete with the yield of methanol, and would lead to gradual loss of reactivity. The evidence does not support involvement of surface hydroxyl groups. First, methanol

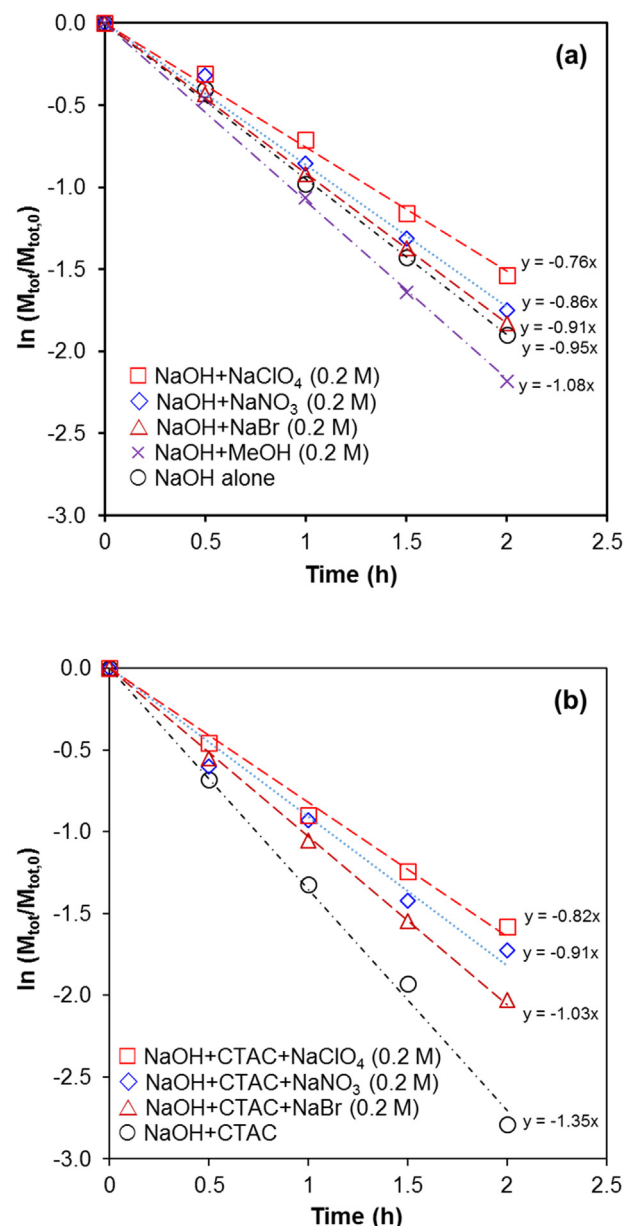


Fig. 7. Effects of different added salts or methanol on the hydrolysis of MeBr adsorbed to 0.5 g WPX-1 in 1 mL of 1 M NaOH in (a) the absence or (b) the presence of 0.1 M cetyltrimethylammonium chloride.

Table 3

Variation with cycle of overall pseudo first-order reaction rate constant of base hydrolysis of MeBr adsorbed to recycled RO activated carbon pellets in 1 M NaOH solution at 55°C with a solid/aqueous volume ratio of 0.5 mg/L.

Cycle	k_{obs} (h^{-1})
1st	0.91 ± 0.04
2nd	0.91 ± 0.09
3rd	0.96 ± 0.05
4th	1.01 ± 0.09
5th	0.92 ± 0.03

and dimethyl ether account for most of the product. Second, the incremental yields of bromide and methanol from WPX-1 were unchanged after four sequential MeBr doses (Fig. S11). Third, a recycling test of granular RO showed no loss of activity after 5 cycles (Table 3). Had surface groups been involved, the rate would

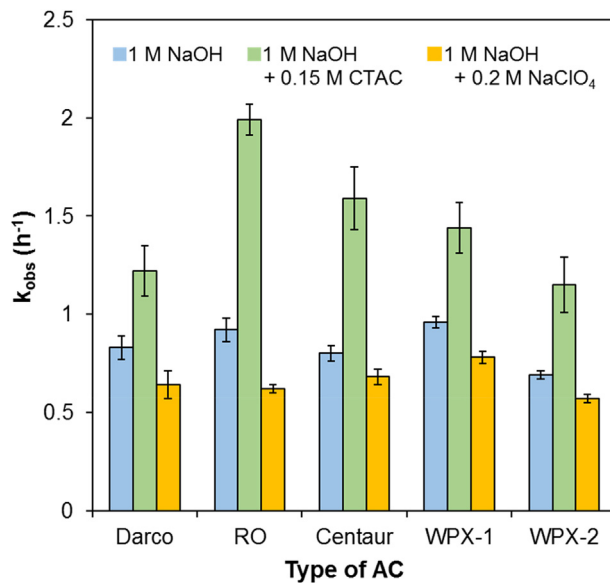


Fig. 8. Effects of CTAC and NaClO₄ on the degradation of AC-adsorbed MeBr by 1 M NaOH under the conditions described in Fig. 4(a) (at loading rate 0.011 g/g).

have decreased and the incremental yield of methanol would have increased with cycle number.

Therefore, the evidence taken as a whole leads us to conclude that the main pathway is direct reaction between adsorbed MeBr and sorbed hydroxide ion. It is left to consider exactly how that occurs. It is recognized that MeBr forms monolayers on AC surfaces as well as condensed, liquid-like phases in nanopores, depending on the chemical potential of MeBr and the pore size distribution of the AC. Because of the high porosity of carbons, the MeBr condensate presents a high interfacial surface area between liquified MeBr and the aqueous phase.

One possible mechanism poses the existence of an aqueous interfacial zone near the liquified MeBr-water boundary where the concentration of MeBr is elevated, and, therefore, hydrolysis is faster compared to the bulk aqueous phase. Since there is no reason to expect competition by other inert anions for hydroxide ion in this zone, this mechanism is inconsistent with the observed inhibitory effect of inert anions.

A second possible mechanism is ion pair partitioning (as Na⁺OH⁻) into the liquified MeBr phase. Partitioning should increase with relative permittivity. Consistent with this mechanism, Table 2 shows that the ratio of rate constants for hydrolysis on the solid phase relative to bulk solution ($k_{\text{obs,AC}}/k_{\text{obs,aq}}$) follows the order, MeBr > EtBr > PrBr, the same as the order in relative permittivity of the liquid phase MeBr (9.71) > EtBr (9.0) > PrBr (8.09) [30]. Also, in keeping with this hypothesis, quaternary ammonium surfactant could accelerate the rate by acting as phase-transfer catalyst for OH⁻, and inert anions could decrease the rate by competing for counterion positions in a quaternary ammonium ion pair. However, experiments described in the SI section show that NaOH from a 1 M aqueous solution does not partition into any of the liquid alkyl bromides appreciably —i.e., the resulting [NaOH] in the organic phase in each case was $<1 \times 10^{-5}$ M. This concentration is too small to explain the observed $k_{\text{obs,AC}}/k_{\text{obs,aq}}$ of 0.13 (for WPX-1) or 0.087 (WPX-2) for the degradation of MeBr by the pristine carbons for the following reason. Under the assumption that most MeBr exists in liquified form in the pores, then in Eqs. (3) and (4), $k_{\text{obs,AC}} = k_{\text{AC}}[\text{OH}^-]_{\text{MeBr}}$, where k_{AC} (h⁻¹ mol⁻¹ L⁻¹ MeBr) is the second-order rate constant in liquified MeBr and $[\text{OH}^-]_{\text{MeBr}}$ (mol L⁻¹ MeBr) is the hydroxide concentration in liquified MeBr. Taking $[\text{OH}^-]_{\text{MeBr}}$ to be 1×10^{-5} mol L⁻¹ MeBr would require that k_{AC} be at least 1.3×10^4 -times (WPX-1) or 8.7×10^3 -times (WPX-

2) greater than k_{aq} , which is unreasonable, given that there is no statistically significant difference between E_a in the aqueous and WPX-1 states (Fig. 2). Thus, the ion pair partitioning mechanism can be ruled out, at least for pristine ACs.

A third possibility, and the one considered most likely, is an anion exchange site (AES) mechanism in which hydroxide ions are attracted to positive sites on the AC surface. The AES is illustrated in Fig. 9. Although the ACs are net negatively charged at high pH, a low density of positively charged sites may exist that provide anion exchange sites for OH⁻. It may be speculated that these positive sites are provided by quaternary heterocyclic N. During pyrolysis, N becomes incorporated in the graphene layers replacing carbon atoms, and after severe pyrolysis some locate in the interiors of the graphene as quaternary-N [31]. Both WPX and RO activated carbons, similar to the ACs used here, were found to contain a small amount of N, some of it in a heat-treated sample being in quaternary form [32–34]. Nevertheless, further study is needed to identify what properties of the carbon contribute to the anion exchange capacity. By the AES mechanism, quaternary ammonium surfactants play the dual role of neutralizing surface negative charge, thereby reducing electrostatic repulsion of OH⁻, and by increasing positive charge density. The latter occurs via the formation of hemimicelles at the surface which contain organocations in excess of what is needed to neutralize the local surface negative charge [35]. The AES hypothesis is supported by several lines of evidence. The anion exchange capacity determined with bromide ion was $95 \pm 16 \mu\text{mol/g}$ for pristine WPX-1, increasing to $430 \pm 21 \mu\text{mol/g-AC}$ for CTA⁺-coated WPX-1. The CTA⁺ coating increased the zeta potential from negative values to positive values, even at pH 9.7 (Fig. S7). Rate enhancement by CTA⁺ reaches a plateau (Fig. 6) at a dose coincident with the maximum sorption capacity of CTA⁺, as determined in independent experiments in water (Fig. S12). Addition of inert anions slows hydrolysis (Fig. 7) by competing with OH⁻ for anion exchange sites. Similar trends of CTA⁺ enhancement and ClO₄⁻ inhibition were observed for EtBr. In 1 M NaOH, the overall pseudo first-order rate constant of WPX-2-adsorbed EtBr increased from $0.049 \pm 0.003 \text{ h}^{-1}$ to $0.100 \pm 0.003 \text{ h}^{-1}$ with the addition of 0.15 M CTAC, and decreased to $0.036 \pm 0.002 \text{ h}^{-1}$ with the addition of 0.2 M NaClO₄ (Fig. S13). The order in $k_{\text{obs,AC}}/k_{\text{obs,aq}}$, MeBr > EtBr > PrBr, may be explained by assuming that the liquid condensate presents a barrier to diffusion of hydroxide ions to positive sites covered by the condensed liquid. This barrier is expected

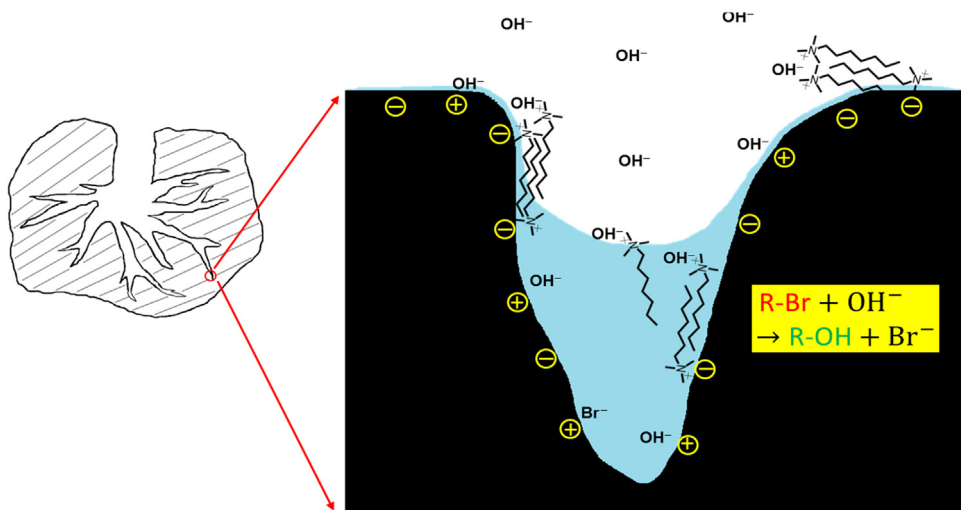


Fig. 9. Proposed AES mechanism for the alkaline hydrolysis of alkyl bromides adsorbed to ACs, in which anion exchange on carbon surface sites controls the degradation rate of alkyl bromides. Black color represents the carbon matrix and blue color represents the alkyl bromide ($R-Br$) adsorbed on the surface or liquefied in a pore. (For interpretation of the references to colour in this figure legend, the reader is referred to the web version of this article.)

to increase with decreasing relative permittivity ($MeBr > EtBr > PrBr$ [30]) and with increasing degree of pore filling at a given alkyl bromide concentration (expected order, $MeBr < EtBr < PrBr$). Consistent with this explanation, addition of 0.15 M CTAC increased $k_{obs,AC}$ of EtBr by 128%, but increased $k_{obs,AC}$ of MeBr by only 86% (Table S1).

3.6. Summary remarks

In this study we have shown that base hydrolysis of methyl bromide in aqueous suspensions of activated carbons occurs both in the dissolved and adsorbed states. Reaction in the adsorbed state is accelerated by treatment of the carbon with cationic surfactants, and is inhibited by competing anions, in accord with an anion exchange site mechanism. The AES mechanism applies to a variety of carbons and to other alkyl bromides, but the contribution of adsorbed-state hydrolysis to higher alkyl bromides compared to methyl bromide is diminished.

The results may prove valuable in designing treatment strategies for removal of methyl bromide from fumigation vent streams. The weak temperature dependence of adsorption mitigates concern about having to raise temperature to achieve satisfactory rates of hydrolysis in practical applications. Hydrolysis products are a consideration in practical application. Bromide at 0.2 M only slightly decreases the rate (Fig. 7a), suggesting that its effect on the rate would not be felt until several cycles had been completed. On the other hand, methanol significantly increases the overall rate of $MeBr$ hydrolysis and the yield of dimethyl ether, which is a gas at ordinary temperatures. The stability of the rate constant after five cycles (Table 3) and the linear relationship between methanol or bromide yield and dose number up to at least four cycles (Fig. S11) are encouraging because they suggest that the carbons are robust even after the buildup of products.

Acknowledgement

This work was supported by a FAS/U.S. Department of Agriculture TASC grant through the California Dried Plum Board.

Appendix A. Supplementary data

Supplementary data associated with this article can be found, in the online version, at <http://dx.doi.org/10.1016/j.apcatb.2017.04.010>.

References

- [1] M.W.I. Schmidt, A.G. Noack, Black carbon in soils and sediments: analysis, distribution, implications, and current challenges, *Glob. Biogeochem. Cycles* 14 (3) (2000) 777–793.
- [2] A.M.P. Oen, B. Beckingham, U. Ghosh, M.E. Kruså, R.G. Luthy, T. Hartnik, T. Henriksen, G. Cornelissen, Sorption of organic compounds to fresh and field-aged activated carbons in soils and sediments, *Environ. Sci. Technol.* 46 (2) (2012) 810–817.
- [3] W. Xu, K.E. Dana, W.A. Mitch, Black carbon-mediated destruction of nitroglycerin and RDX by hydrogen sulfide, *Environ. Sci. Technol.* 44 (16) (2010) 6409–6415.
- [4] Y.-F. Li, M.-Q. Guo, S.-F. Yin, L. Chen, Y.-B. Zhou, R.-H. Qiu, C.-T. Au, Graphite as a highly efficient and stable catalyst for the production of lactones, *Carbon* 55 (2013) 269–275.
- [5] F. Begum, H. Zhao, S.L. Simon, Modeling methyl methacrylate free radical polymerization: reaction in hydrophobic nanopores, *Polymer* 53 (15) (2012) 3261–3268.
- [6] F. Rodríguez-reinoso, The role of carbon materials in heterogeneous catalysis, *Carbon* 36 (3) (1998) 159–175.
- [7] K. Mackenzie, J. Battke, F.D. Kopinke, Catalytic effects of activated carbon on hydrolysis reactions of chlorinated organic compounds: part 1. γ -Hexachlorocyclohexane, *Catal. Today* 102–103 (2005) 148–153.
- [8] K. Mackenzie, J. Battke, R. Koehler, F.D. Kopinke, Catalytic effects of activated carbon on hydrolysis reactions of chlorinated organic compounds: part 2. 1,1,2,2-Tetrachloroethane, *Appl. Catal. B: Environ.* 59 (2005) 171–179.
- [9] W. Chen, Y. Li, D. Zhu, S. Zheng, W. Chen, Dehydrochlorination of activated carbon-bound 1,1,2,2-tetrachloroethane: implications for carbonaceous material-based soil/sediment remediation, *Carbon* 78 (2014) 578–588.
- [10] M.F.R. Pereira, J.J.M. Órfão, J.L. Figueiredo, Oxidative dehydrogenation of ethylbenzene on activated carbon catalysts. I. Influence of surface chemical groups, *Appl. Catal. A: Gen.* 184 (1) (1999) 153–160.
- [11] H.J. Amezquita-García, E. Razo-Flores, F.J. Cervantes, J.R. Rangel-Mendez, Activated carbon fibers as redox mediators for the increased reduction of nitroaromatics, *Carbon* 55 (2013) 276–284.
- [12] W. Xu, J.J. Pignatello, W.A. Mitch, Reduction of nitroaromatics sorbed to black carbon by direct reaction with sorbed sulfides, *Environ. Sci. Technol.* 49 (6) (2015) 3419–3426.
- [13] H.M. Heilmann, U. Wiesmann, M.K. Stenstrom, Kinetics of the alkaline hydrolysis of high explosives RDX and HMX in aqueous solution and adsorbed to activated carbon, *Environ. Sci. Technol.* 30 (5) (1996) 1485–1492.
- [14] J. Gan, N.E. Megonell, S.R. Yates, Adsorption and catalytic decomposition of methyl bromide and methyl iodide on activated carbons, *Atmos. Environ.* 35 (5) (2001) 941–947.
- [15] A. Georgi, U. Trommler, A. Reichl, F.-D. Kopinke, Influence of sorption to dissolved humic substances on transformation reactions of hydrophobic organic compounds in water. Part II: hydrolysis reactions, *Chemosphere* 71 (8) (2008) 1452–1460.

[16] U.N.E. Programme, European Community Management Strategy for the Phase-out of the Critical Uses of Methyl Bromide, 2009, http://ozone.unep.org/Exemption_Information/Critical_use_nominations_for_methyl.bromide/MeBr_Submissions/EC%20Management%20Strategy%20for%20Methyl%20Bromide.pdf (Accessed 11/1/2016).

[17] J.P. Wood, M.J. Clayton, T. McArthur, S.D. Serre, L. Mickelsen, A. Touati, Capture of methyl bromide emissions with activated carbon following the fumigation of a small building contaminated with a *Bacillus anthracis* spore simulant, *J. Air Waste Manag. Assoc.* 65 (2) (2015) 145–153.

[18] J.D. Snyder, J.G. Leesch, Methyl bromide recovery on activated carbon with repeated adsorption and electrothermal regeneration, *Ind. Eng. Chem. Res.* 40 (13) (2001) 2925–2933.

[19] Y. Yang, Y. Li, S.S. Walse, W.A. Mitch, Destruction of methyl bromide sorbed to activated carbon by thiosulfate or electrolysis, *Environ. Sci. Technol.* 49 (7) (2015) 4515–4521.

[20] J. Gan, S.R. Yates, Recapturing and decomposing methyl bromide in fumigation effluents, *J. Hazard. Mater.* 57 (1–3) (1998) 249–258.

[21] A. Streitwieser, *Solvolytic Displacement Reactions*, McGraw-Hill book company, Inc., New York N.Y., 1962.

[22] R.P. Schwarzenbach, P.M. Gschwend, D.M. Imboden, *Environmental Organic Chemistry*, 2nd edition, John Wiley & Sons, Inc, Hoboken, New Jersey, 2002.

[23] L.W. Zelazny, L. He, A. Vanwormhoudt, Charge analysis of soils and anion exchange, in: D.L. Sparks, A.L. Page, P.A. Helmke, R.H. Loepert (Eds.), *Methods of Soil Analysis Part 3—Chemical Methods*, Soil Science Society of America, American Society of Agronomy, Madison, WI, 1996, pp. 1231–1253.

[24] R. Xuan, D.J. Ashworth, L. Luo, H. Wang, S.R. Yates, Depleting methyl bromide residues in soil by reaction with bases, *Environ. Sci. Technol.* 44 (23) (2010) 9080–9085.

[25] A.R.S. United States Department of Agriculture, Henry's Law Constant for Methyl Bromide as a Function of Temperature, 2005, <http://www.ars.usda.gov/News/docs.htm?docid=10408&page=5> (Accessed 6/3/2016).

[26] T.B. Phan, H. Mayr, Comparison of the nucleophilicities of alcohols and alkoxides, *Can. J. Chem.* 83 (9) (2005) 1554–1560.

[27] P. Hou, F.S. Cannon, N.R. Brown, T. Byrne, X. Gu, C.N. Delgado, Granular activated carbon anchored with quaternary ammonium/epoxide-forming compounds to enhance perchlorate removal from groundwater, *Carbon* 53 (2013) 197–207.

[28] X. Wang, C. Feng, N. Ding, Q. Zhang, N. Li, X. Li, Y. Zhang, Q. Zhou, Accelerated OH-transport in activated carbon air cathode by modification of quaternary ammonium for microbial fuel cells, *Environ. Sci. Technol.* 48 (7) (2014) 4191–4198.

[29] H.P. Gregor, J. Belle, R.A. Marcus, Studies on ion-exchange resins. XIII. Selectivity coefficients of quaternary base anion-exchange resins toward univalent anions, *J. Am. Chem. Soc.* 77 (10) (1955) 2713–2719.

[30] W.M. Haynes, D.R. Lide, T.J. Bruno, *CRC Handbook of Chemistry and Physics*, 94th edition, Taylor & Francis Group, LLC, Boca Raton, FL, 2013.

[31] J.R. Pels, F. Kapteijn, J.A. Mouljin, Q. Zhu, K.M. Thomas, Evolution of nitrogen functionalities in carbonaceous materials during pyrolysis, *Carbon* 33 (11) (1995) 1641–1653.

[32] P. Pourrezaei, A. Alpatova, P. Chelme-Ayala, L.A. Perez-Estrada, M. Jensen-Fontaine, X.C. Le, M. Gamal El-Din, Impact of petroleum coke characteristics on the adsorption of the organic fractions from oil sands process-affected water, *Int. J. Environ. Sci. Technol.* 11 (7) (2014) 2037–2050.

[33] J.L. Figueiredo, M.F.R. Pereira, M.M.A. Freitas, J.J.M. Órfão, Modification of the surface chemistry of activated carbons, *Carbon* 37 (9) (1999) 1379–1389.

[34] A. Świątkowski, M. Pakula, S. Biniak, M. Walczyk, Influence of the surface chemistry of modified activated carbon on its electrochemical behaviour in the presence of lead(II) ions, *Carbon* 42 (15) (2004) 3057–3069.

[35] H.-J. Hong, H. Kim, Y.-J. Lee, J.-W. Yang, Removal of anionic contaminants by surfactant modified powdered activated carbon (SM-PAC) combined with ultrafiltration, *J. Hazard. Mater.* 170 (2–3) (2009) 1242–1246.